NJC

Accepted Manuscript

ROYAL SOCIETY OF CHEMISTRY

rsc.li/njc

View Article Online
DOI: 10.1039/C7NJ02557B

NJC

PAPER

Biosynthesized Pd/γ-Al_2O_3 catalysts for low-temperature 1,3-butadiene hydrogenation: Effect of calcination atmosphere

Received 00th January 20xx,
Accepted 00th January 20xx

DOI: 10.1039/x0xx00000x

www.rsc.org/

Fenfen Lu,[a] Yan Xu,[b] Xia Jiang,[b] Yang Liu,[b] Jiale Huang[b] and DaohuaSun*[,b]

Low temperature 1,3-butadiene hydrogenation over biosynthesized Pd/γ-Al_2O_3 catalysts annealed under different atmosphere (H_2, Air) was compared in a fixed bed reactor, and the catalysts were prepared with a facile sol-immobilization method. The structural properties of Pd/γ-Al_2O_3 catalysts in relation to their activities on 1,3-butadiene hydrogenation were investigated through the information of the X-ray photoelectron spectroscopy, X-ray diffraction, hydrogen temperature-program reduction, thermogravimetry, transmission electron microscopy, CO chemisorption measurements techniques and Fourier transform infrared spectroscopy. The results of characterizations revealed that calcination atmosphere (H_2, Air) exhibited remarkable impact on the chemical state of Pd species and catalytic activity, and the coexistence of the metallic state and oxidation state state of Pd was a key factor for the higher catalytic activity and butene selectivity, while the catalyst with existence of the metallic state only (H_2-Pd/γ-Al_2O_3) showed lower butene selectivity, and the catalyst with oxidation state state alone (Air-Pd/γ-Al_2O_3) hardly show active in 1,3-butadiene hydrogenation. Therefore, the chemical state of Pd played an important role for 1,3-butadiene hydrogenation reaction.

Introduction

Selective hydrogenation is one of the critical reactions to remove alkynes or alkadienes in the stream for polymer synthesis[1]. For further polymerization processing, the level of impurity must be reduced to below 10 ppm, otherwise they would poison the catalysts and degrade the product quality[1-3]. To overcome the problems, the alkynes or alkadienes should be catalytically converted to alkenes in order to avoid hydrogenation of the alkene stream[3]. Palladium (Pd) is so far regarded as the unique metal, have been widely applied for hydrogenation reactions and in particular for selective partial hydrogenation of alkadienes or alkynes[4, 5]. Typically, hydrogenation of 1,3-butadiene is used for the purification of butene streams. For instance, Bachiller-Baeza et al found that Pd catalysts supported on different types of nanofibers with different graphitic structure show excellent performance in the partial hydrogenation of 1,3-butadiene, and selectivity to butenes higher than 95% were obtained with the catalysts prepared on SO_3H-modified supports or with the $PdSO_4$ precursor[6].

Catalysts pretreated with different atmospheres were usually carried out to improve the catalytic performance before the activity test. In general, two main pretreatment methods have been reported[7-9], reducing atmosphere (e.g. hydrogen containing atmosphere) and oxidation atmosphere (e.g. oxygen containing atmosphere). As reported, the influence mechanism of pretreatment mostly focused on changing the chemical state of the active species[7, 10-13], particle size[14, 15], texture and structure of Pd catalysts[16]. Suresh et al. obtained Pd particles with size as close as possible to that observed in equilibrated active catalysts (80-100 nm) by using different calcination procedures, and found that metal crystallites of about 40 nm agglomerate up to 150 nm in helium atmosphere and to even larger size in H_2/He[14]. Skoda et al. found that there were no significant modifications of the Pd catalyst structure under whatever the atmosphere (oxygen or hydrogen). Generally speaking, the chemical state of Pd can be divided into three groups, namely the metallic state (Pd^0), the oxidized sate (PdO/Pd^{2+}) and a mixture of both states ($Pd^0/PdO/Pd^{2+}$), depending on the catalytic process[17-19]. Many researchers considered that Pd^0 of the catalyst is more active than PdO/Pd^{2+} for some reactions[7]. For example, Chesnokov et al. found that Pd^0 shown better performance, when increasing the fraction of Pd^{2+} result in the decrease of both total activity and selectivity of Pd/C catalysts in the selective hydrogenation of 1,3-butadiene[20]. However, Saldan et al. considered that mixed-valent states of Pd lead to a powerful colloidal catalyst[21]. Although the catalytic performance of supported Pd catalysts has been widely investigated in hydrogenation, the exact active chemical state is still controversial. Thus, it is important to understand the effect of the surface state of supported Pd catalysts on the catalytic reaction, and the main goal of this work was to examine the influence of

[a] College of Chemistry & Materials Science, Longyan University, Longyan, 364012, PR China.
[b] Department of Chemical and Biochemical Engineering, College of Chemistry and Chemical Engineering, Fujian Provincial Key Laboratory of Chemical Biology, Xiamen University, Xiamen, 361005, PR China.
Email: sdaohua@xmu.edu.cn

† Electronic Supplementary Information (ESI) available: [details of any supplementary information available should be included here]. See DOI: 10.1039/x0xx00000x

View Article Online
DOI: 10.1039/C7NJ02557B

pretreatment conditions on the adsorption and catalytic activities of 1,3-butadiene hydrogenation over the supported Pd catalyst.

Biosynthesized metal catalysts have received increasing attention in the past decade, as an emerging highlight of the intersection of biotechnology and nanotechnology[22-25]. In this work, the Pd nanoparticles were obtained by the reduction of palladium nitrate with the extract of *Cacumen platycladi* (*C.P.*) leaves, which supported on γ-Al_2O_3 by sol-immobilization (SI) method[24]. Detailed studies on structure of Pd/γ-Al_2O_3 catalyst prepared by biological method under different calcination atmosphere (H_2 and Air) was investigated systematically and discussed. The X-ray photoelectron spectroscopy (XPS), X-ray diffraction (XRD), transmission electron microscopy (TEM), thermogravimetry (TG), hydrogen temperature-program reduction (H_2-TPR), CO chemisorptions measurements techniques and Fourier transform infrared spectroscopy (FTIR) were adopted to study the reaction of 1,3-butadiene hydrogenation with the biosynthesized Pd catalysts.

Experimental

Catalyst preparation

Sundried *C.P.* leaves were purchased from Xiamen Jiuding Drugstore (China). Palladium nitrate ($Pd(NO_3)_2$) was purchased from Aladdin Reagent Co. Ltd. (China) and used as received. The *C.P.* leaves were milled and 1.0 g of the milled powder was dispersed in 250 mL conical flask with 100 mL deionized water and kept in a water bath shaker at 30 °C. After 2 h, the mixture was filtered to obtain the extract.

10 mL aqueous solution of $Pd(NO_3)_2$ (1.0 mM of the concentration of metal) was heated to 90 °C in an oil bath with a constant temperature and a stirring rate of 600 rpm. Subsequently, 10 mL of the *C.P.* leaves extract was added to this precursor solution with vigorous stirring for 1 h. Then, weighed amount of γ-Al_2O_3 support was added into the as-formed hydrosol (to keep the metal concentration 0.5 wt %), and HNO_3 was also added to maintain the pH value at around 2. After the mixture being stirred vigorously for another 1 h, the suspension was filtered through a cellulose filter membrane with the pore size 0.8 mm. The filter residue was washed three times with deionized water, and finally dried in a vacuum oven at 50 °C for 12 h, and the responding catalysts were labeled as Fresh-Pd/γ-Al_2O_3. The as-prepared catalyst was calcined at 350 °C in H_2 or air atmosphere for 4 h with a ramp rate of 5 °C/min. These two samples were denoted as H_2-Pd/γ-Al_2O_3 and Air-Pd/γ-Al_2O_3, respectively.

Catalyst characterization

The dried and powdered samples were then analyzed via XRD using an X-ray diffractometer (Phillips, Netherlands) with Cu Kα radiation (40 kV, 30 mA). XPS characterization was obtained on a PHI-Quantum 2000 spectrometer. And the catalysts were characterized by X-ray equipped with a hemispherical electron analyzer and an Al Kα (1486.6 eV) X-ray source. Samples for TEM were prepared by placing a drop of as prepared hydrosol on carbon-coated copper grids and allowing water to completely evaporate. TEM samples were observed on a Tecnai F30 Microscope. TG studies were carried out on a SDTQ600 thermo balance under flowing air atmosphere at a heating rate of 10 °C/min.

H_2-TPR was performed with a Micromeritics AutoChem II 2920 chemisorption analyzer. Samples (100 mg) were weighed, 10 % H_2/90 % N_2 was flowed through the samples while the temperature was increased from 30 °C to 800 °C (heating rate: 10 °C/min). The thermal conductivity detector signal automatically recorded the H_2 consumption. The specific surface area of catalysts was measured by N_2 adsorption using a Micromeritics Tristar II 3020 instrument. The surface area was calculated using the Brunauer Emmett Teller, and the total pore volume was obtained by the single point desorption at P/P_0 = 0.99. The average pore diameter was determined using the Barrett Joyner Halenda (BJH) method as applied to the desorption branch of the isotherms. The *in situ* FTIR experiments were performed using a home-built *in situ* IR cell with quartz lining and CaF_2 windows in a Nicolet 6700 FTIR spectrometer using an MCT/A detector. Prior to the adsorption experiment, the samples were pretreated *in situ* at 35 °C in a vacuum. The spectra of the samples at 35 °C prior to the adsorption were used as background in a vacuum.

Catalyst testing

The hydrogenation of 1,3-butadiene was carried out at 35 °C in a fixed-bed flow stainless reactor (inner diameter: six mm) under atmospheric pressure. The temperature of hydrogenation reaction was measured by using a glass tube covered Cr-Al thermocouple located in the center of the catalyst bed. 50 mg of catalyst was weighted and loaded into the reactor; the feed flow rate was adjusted to 13.5 mL/min with mass flowmeter (Seven star Electronics), which contained a mixture of 2.15% 1,3-butadiene, 4.30 % H_2, and balance with N_2. The reactor effluent was analyzed on line using a gas chromotograph (GC) equipped with an Al_2O_3 column and an FID detector.

The product stream was sampled every 20 min and then analyzed. Conversion and selectivity determined from the GC were corresponding to the reactant (1,3-butadiene), main products (1-butene, cis-2-butene and trans-2-butene) and side product (butane).

Results and Discussion

1,3-butadiene hydrogenation over the Pd/γ-Al_2O_3 catalysts

The catalytic performance for 1,3-butadiene hydrogenation over the Pd/γ-Al_2O_3 catalysts prepared under different calcinations atmospheres was shown in Fig. 1. Obviously, the calcination atmospheres dramatically influenced the catalytic performances for the three catalysts. The Fresh-Pd/γ-Al_2O_3 catalyst showed the best catalyst performance among all the samples, namely, the conversion of 1,3-butadiene was 100% and the selectivity of butene was 51.2%. As for H_2-Pd/γ-Al_2O_3, the selectivity decreased to 8.7%, and the conversion remained the same. However, Air-Pd/γ-Al_2O_3 hardly showed activity in 1,3-butadiene hydrogenation. To further clarify the influence of the calcination atmosphere on the structure,

View Article Online
DOI: 10.1039/C7NJ02557B
NJC Paper

particle sizes, surface state and hydrogenation property of catalysts, a series of characterizations have been employed.

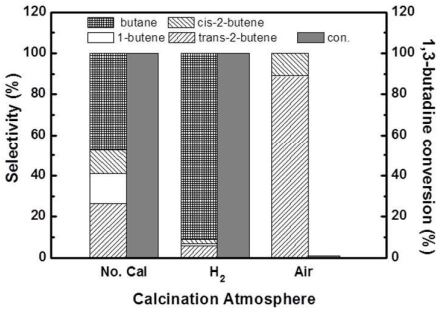

Fig. 1 Effect of different calcination atmosphere on the activity of 1,3-butadiene hydrogenation.

Characterization of catalysts

Fig. 2 shows the N_2 adsorption-desorption isotherms and pore diameter distributions of Pd/γ-Al_2O_3 catalysts without calcination and calcined under H_2 or air, respectively. It is so obviously that, these three catalysts still remained typical IV adsorption-desorption isotherms with H1-type hysteresis, indicating that the porous structures of γ-Al_2O_3 were not deteriorated[12]. The physical properties of all catalysts were summarized in Table 1. After Pd immobilization, the surface area and the pore volume decreased, in comparison with those of the pristine γ-Al_2O_3, showing that the nanoscale Pd nanoparticles have been successfully supported into the pore structure of the γ-Al_2O_3. While the pore diameter became lager instead, owning to the Pd nanoparticles in the pore had the pore expanding effect[26]. After pretreated with different atmosphere, the surface area and the pore volume of H_2-Pd/γ-Al_2O_3 and Air-Pd/γ-Al_2O_3 became larger than that of Fresh-Pd/γ-Al_2O_3, the crack and vaporization of the remaining biomolecules in the pore of catalysts may responsible for this

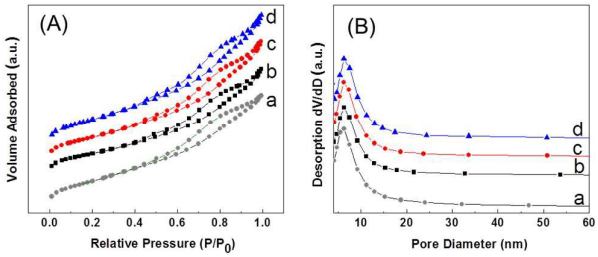

Fig. 2 N_2 adsorption-desorption isotherms (A) and pore size distribution (B) of Pd/γ-Al_2O_3 catalysts: (a) γ-Al_2O_3, (b) Fresh-Pd/γ-Al_2O_3, (c) H_2-Pd/γ-Al_2O_3 and (d) Air-Pd/γ-Al_2O_3.

Table 1
The structural properties of Pd/γ-Al_2O_3 catalysts pretreated under different atmospheres.

Samples	BET[a] (m^2/g)	V[b] (cm^3/g)	D[c] (nm)
γ-Al_2O_3	203	0.32	5.3
Fresh-Pd/γ-Al_2O_3	180	0.30	5.8
H_2-Pd/γ-Al_2O_3	199	0.33	5.8
Air-Pd/γ-Al_2O_3	230	0.37	5.8

[a] BET specific surface.
[b] Total pore volume.
[c] The pore diameter calculated from the desorption branch of the isotherm using the BJH method.

phenomenon. Moreover, the total pore diameter of all catalysts was almost in the same range. That was to say, pretreatment of the catalysts had negligible effect on the physical structure of Pd catalysts. Meanwhile, this can also be achieved in the thermo gravimetric analysis shown in Fig. 3. According to the TG profile, the main weight loss was between 200 °C and 500 °C, the weight loss at 200 °C was attributed to the decrease of some volatile compound, and the weight loss at 400 °C was due to crack and vaporization of the organic molecules[26]. Therefore, in comparison with the Fresh-Pd/γ-Al_2O_3, there still remained some biomolecules on the surface of Pd/γ-Al_2O_3 catalyst after calcination under H_2 or air at 350 °C. Particularly, Air-Pd/γ-Al_2O_3 possesses the least residual biomolecules, which was in accordance with the variation trend of the surface area and pore volume.

The TEM images of the Pd/γ-Al_2O_3 catalysts calcined at different atmosphere were shown in Fig. 4. For the Fresh-Pd/γ-Al_2O_3 catalyst, the Pd nanoparticles were fairly well dispersed and had the average particle size of 7.4±0.5 nm (Fig. 4A). After calcined in hydrogen atmosphere, the particle size of H_2-Pd/γ-Al_2O_3 almost stayed the same, 7.5±0.6 nm (Fig. 4B). And the particle size increased slightly to 8.3±0.4 nm (Fig. 4C) for the Air-Pd/γ-Al_2O_3 sample according to histogram analysis. The results showed that after annealing in different atmosphere, the particle size of catalysts were not changed obviously, but The catalytic performance of these three catalysts for 1,3-butadiene hydrogenation were greatly different. That was to say, after calcined, there may be some other differences among these catalysts, leading to the varied performance in reaction.

The binding energy (BE) of electrons determined by XPS provides useful information on the chemical states of different elements of the catalysts in different atmosphere[27]. Therefore,

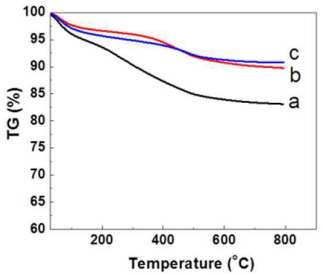

Fig. 3 TG profiles of (a) Fresh-Pd/γ-Al_2O_3, (b) H_2-Pd/γ-Al_2O_3 and (c) Air-Pd/γ-Al_2O_3.

View Article Online
DOI: 10.1039/C7NJ02557B

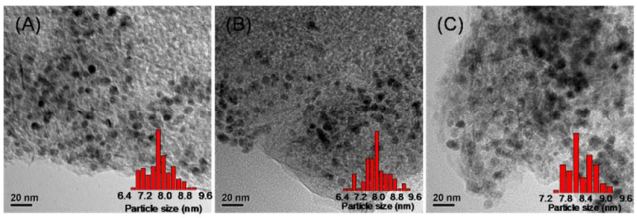

Fig. 4 TEM images and size histograms (inlet) of (A) Fresh-Pd/γ-Al_2O_3, (B) H_2-Pd/γ-Al_2O_3 and (C) Air-Pd/γ-Al_2O_3.

we used XPS analysis to measure surface properties of the fresh catalyst and the calcined catalysts in H_2 and air atmospheres. The XPS peak deconvolution results of the samples were presented in Fig. 5. For H_2-Pd/γ-Al_2O_3 catalyst, the BE value of $Pd_3d_{5/2}$ and $Pd_3d_{3/2}$ were found to be around 334.9 eV and 340.2 eV respectively, such values indicated the presence of metallic Pd state[28, 29]. As for Air-Pd/γ-Al_2O_3 catalyst, the BE value of $Pd_3d_{5/2}$ and $Pd_3d_{3/2}$ were found to be around 336.5 eV and 341.8 eV, respectively, which corresponding to oxidation state[30, 31]. However, as for the Fresh-Pd/γ-Al_2O_3 catalyst, the BE value of $Pd_3d_{5/2}$ and $Pd_3d_{3/2}$ were around 336.0 eV and 341.3 eV, respectively, the peaks were broad and can be broken up into two peaks, which belong to the chemical state of PdO/Pd^{2+} and Pd^0 species in the Fresh-Pd/γ-Al_2O_3 catalyst. After H_2 pretreatment, the BE values of the Pd decreased by 1.1 eV, only Pd^0 was present on the surface, which proved that all the Pd metal have been restored to zero valence state after calcined in hydrogenation atmosphere. After air pretreated, the BE values of Pd increased slightly, since the oxidation of Pd^0 to PdO/Pd^{2+} during the pretreatment process, and only PdO/Pd^{2+} was present on the surface of Air-Pd/γ-Al_2O_3. In addition, comparing the hydrogenation performance of these three catalysts, the conversion of 1,3-butadiene by Fresh-Pd/γ-Al_2O_3 and H_2-Pd/γ-Al_2O_3 catalysts was up to 100%, while Air-Pd/γ-Al_2O_3 catalyst was mostly inactive. We can speculate that Pd^0 was the active side for 1,3-butadiene hydrogenation. Since the particle diameter of the three (7.4±0.5, 7.5±0.6 and 8.3±0.4 nm) was basically the same, thus the chemical state of palladium was one of the most important factors for the hydrogenation of 1,3-butadiene, and the coexistence of Pd^0 and PdO/Pd^{2+} was beneficial for the hydrogenation reaction[21].

Fig. 6 shows the powder XRD patterns of the calcined and fresh catalyst samples. The sharp peaks of the Fresh-Pd/γ-Al_2O_3 (curve a) and H_2-Pd/γ-Al_2O_3 (curve b) catalysts at 40.0° (2θ) was assigned to the (111) plane of crystalline Pd (ICCD, PDF2: 00-046-1043), indicating that the obvious existence of metallic Pd in these two catalysts. Obviously, no distinct change in XRD patterns could be observed after treating the samples with H_2, which showed that the crystal phase of the

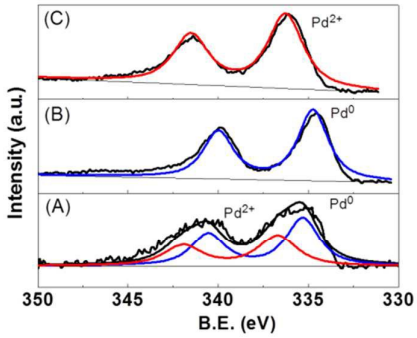

Fig. 5 XPS spectra recorded from the catalysts of (A) Fresh-Pd/γ-Al_2O_3, (B) H_2-Pd/γ-Al_2O_3 and (C) Air-Pd/γ-Al_2O_3.

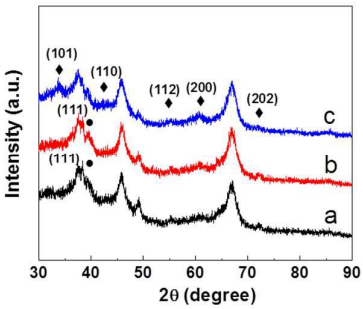

Fig. 6 XRD patterns of Pd/γ-Al_2O_3 catalysts pretreated under different atmospheres: (a) Fresh-Pd/γ-Al_2O_3, (b) H_2-Pd/γ-Al_2O_3, and (c) Air-Pd/γ-Al_2O_3 ((◆) diffraction of PdO, and (●) diffraction of Pd).

active species was similar to that of the Fresh-Pd/γ-Al_2O_3 catalyst. According to the Air-Pd/γ-Al_2O_3 (curve c) catalyst, diffraction peaks at 33.9°, 42.0°, 54.8°, 60.8° and 71.3°, which belonged to the (101), (110), (112), (200) and (202) planes of crystalline PdO/Pd^{2+} (ICCD, PDF2: 00-006-0515), were observed, while metallic state Pd diffraction peaks disappeared. This phenomenon could be attributed to the oxidation of metallic Pd to PdO/Pd^{2+}, which was in accordance with the XPS analysis. No diffraction peaks of PdO could be observed in Fresh-Pd/γ-Al_2O_3, which might be attributed to the low level and high dispersion of PdO species[7, 31]. Apart from the well resolved peaks, no other specific diffraction peaks of Pd were observed in the patterns because of the strong reflections peaks of γ-Al_2O_3 structures. According to the XRD analysis, the presence of the metallic Pd was beneficial for catalytic activity for the hydrogenation. However, the catalyst was inactive when metallic Pd was all oxidized to PdO.

H_2-TPR is a very useful technology to investigate the redox properties and phase composition of the catalysts[12, 32]. The results of the H_2-TPR performance on three Pd/γ-Al_2O_3 catalysts were shown in Fig. 7. Only a negative peak observed at 60-100 °C for all samples due to the formation of PdHx, which were easily reduced to metallic Pd. In this work, the negative peaks of the calcined samples were hardly shift compared with that of Fresh-Pd/γ-Al_2O_3, and the intensity of

View Article Online
DOI: 10.1039/C7NJ02557B

the peaks of calcined samples was higher than that of Fresh-Pd/γ-Al_2O_3. It has been proposed that the decreasing of

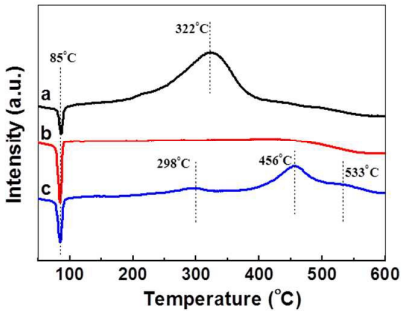

Fig. 7 H_2-TPR profiles of Pd/γ-Al_2O_3catalysts: (a) Fresh-Pd/γ-Al_2O_3, (b) H_2-Pd/γ-Al_2O_3 and (c) Air-Pd/γ-Al_2O_3.

reduction temperature and the intensity of the negative peak were related to the higher Pd dispersion[28, 33], and the result suggested that Fresh-Pd/γ-Al_2O_3 catalyst exhibited better dispersity, which was in accordance with the TEM analysis. Also, it has been reported that the existence of the negative peak may easily cause further hydrogenation for unsaturated carbon-carbon double bond[34], and H_2-Pd/γ-Al_2O_3 has the highest intensity of the negative peak, resulting in the further hydrogenation of 1,3-butadiene to butane. The H_2-TPR profile of Fresh-Pd/γ-Al_2O_3 sample showed a peak at around 322 °C, which can be related to dispersed Pd-oxide in isolated patched, PdOx, on alumina[27, 33]. The H_2-TPR profile of Air-Pd/γ-Al_2O_3 sample showed redox peaks at 298, 456 and 533 °C. The redox peak at 298 °C may belong to the reduction of support interacted PdO species, and the high temperature reduction peak could be a result of reduction of a two-dimensional (2D) PdO surface phase[27]. There were no other H_2 uptake peaks found in the sample of H_2-Pd/γ-Al_2O_3, after calcined under H_2, all Pd species were reduced to Pd^0.

FTIR was also employed to identify the structure of the Pd/γ-Al_2O_3 catalysts, with the typical adsorption spectra in Fig. 8. Compared with the Fresh-Pd/γ-Al_2O_3 sample, the strength of the adsorption peak at 3440 cm^{-1} and 1637 cm^{-1} become weaker, and the peak at 1385 cm^{-1} disappeared. The peak at 1385 cm^{-1} and 3440 cm^{-1} belongs to the stretching vibration of –OH in alcohols and phenolic compounds, and the band at 1637 cm^{-1} can be attributed to the stretching vibrations of (NH)C=O groups, which were responsible for the reduction and stabilization of the Pd nanoparticles during catalysts preparation[35]. After calcination, these peaks were diminished or completely disappeared. Therefore, we can speculate that some biomolecules on the surface of the Pd/γ-Al_2O_3 catalysts has been burnt off after calcination, which was consistence with the analysis results of TG.

To further measure the Pd metal active sites, we focused on *in-situ* FTIR study of CO adsorption on the supported Pd catalysts at room temperature. Fig. 9A shows the FTIR spectra in the 2300-1700 cm^{-1} region of the samples interactions with CO at room temperature. From previous studies[36-38], the peaks observed in FTIR-CO results correspond to various CO species adsorbed on Pd^0. The linear CO species can be observed at

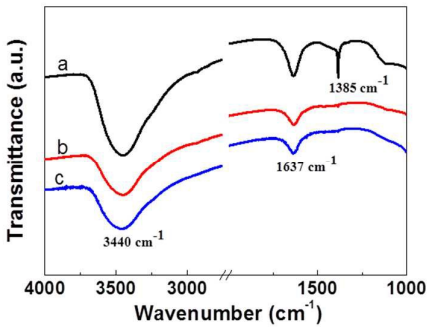

Fig. 8 FTIR spectra of Pd/γ-Al_2O_3 catalysts: (a) Fresh-Pd/γ-Al_2O_3, (b) H_2-Pd/γ-Al_2O_3 and (c) Air-Pd/γ-Al_2O_3.

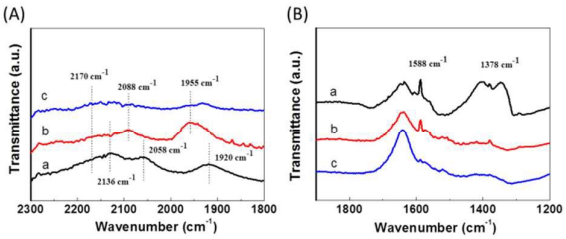

Fig. 9 *In situ* FTIR spectra of CO (A) or 1,3-butadiene (B) absorbed on the Pd/γ-Al_2O_3 catalysts: (a) Fresh-Pd/γ-Al_2O_3, (b) H_2-Pd/γ-Al_2O_3 and (c) Air-Pd/γ-Al_2O_3.

around 2100 cm^{-1}, and IR band below 2000 cm^{-1} were ascribed to the bridge CO species consisting of isolated bridged species, compressed bridged species and three metal bridged species. A weak band at around 2170 cm^{-1} was observed for all samples indicating that some CO interacted with unsaturated Al^{3+} ions[37-39]. Based on the Fig. 9A and references[40], the peak at 2088 cm^{-1} (curve b) and 2058 cm^{-1} (curve a) belonged to linear CO species on Pd(111), while the peak at 1955 cm^{-1} (curve b) and 1920 cm^{-1} (curve a) belonged to bridged CO species on Pd(111). Compared these peaks, we could speculate that H_2-Pd/γ-Al_2O_3 contain more adsorbed Pd^0 species than Fresh-Pd/γ-Al_2O_3. Moreover, there was a peak at 2136 cm^{-1} on Fresh-Pd/γ-Al_2O_3 catalyst, which could be assigned to linear CO species on Pd^{2+}. The existence of the oxidative Pd metal may dilute the metallic Pd active sites in some degree, and then limit the further hydrogenation of butene, which may be the reason for that Fresh-Pd/γ-Al_2O_3 has higher selectivity than H_2-Pd/γ-Al_2O_3. However, there was no apparent peaks among 1800-2300 cm^{-1} for Air-Pd/γ-Al_2O_3, which may be due to that this catalyst have no CO adsorption site. Moreover, Air-Pd/γ-Al_2O_3 hardly showed active in 1,3-butadiene hydrogenation, the possible reason may be that this catalyst has also no 1,3-butadiene adsorption site.

To further measure the adsorption sites of 1,3-butadiene on the Pd catalysts, FTIR study of 1,3-butadiene adsorption on supported Pd catalysts at 35 °C (Fig. 9B). Under the condition of vacuum, only strong adsorption can be detected[41]. As shown in Fig. 9B, A band at around 1588 cm^{-1} was observed for the fresh and H_2 pretreated samples, which was ascribed to the vibrational mode of C=C-C=C. However, this band

View Article Online
DOI: 10.1039/C7NJ02557B

disappeared in the support and the Air-Pd/γ-Al_2O_3 samples. The possible reason for the Air-Pd/γ-Al_2O_3 hardly showed active in 1,3-butadiene hydrogenation reaction may be that there were no 1,3-butadiene adsorption site. Comparing the adsorption results of these three catalysts, it was manifested that the adsorption of the 1,3-butadiene was beneficial for the hydrogenation reaction.

In a word, we can speculate that part of biomolecules remains on the surface of the Pd/γ-Al_2O_3 catalysts after calcination. The active size for 1,3-butadiene hydrogenation was metallic Pd, when increasing in the fraction of Pd^0 in the catalyst composition result in the further hydrogenation. Moreover, as reported before[22, 26], the biomolecule had negative influence on the performance of catalysts, which had been removed to enhance the catalytic activity, since the active site may be covered. So, we speculated the better catalytic performance over Fresh-Pd/γ-Al_2O_3 was largely attributed to the coexistence between Pd^0 and PdO/Pd^{2+} species.

Conclusions

In conclusion, we have reported the effect of oxidative and reductive atmosphere pretreatment on the catalytic performance of Pd/γ-Al_2O_3 catalysts for 1,3-butadiene hydrogenation. It is found that there were no obvious differences between the fresh Pd catalyst and the calcined catalysts under different (H_2 and air) atmospheres in physical structure, and the particle diameter of these three catalysts (7.4±0.5, 7.5±0.6 and 8.3±0.4 nm) was basically the same, but the chemical state of Pd varied greatly, there only metallic Pd species after calcination under H_2 atmosphere, while calcined under air atmosphere, catalyst existing mainly in the oxide form. Therefore, we speculated that the metallic Pd was the active specie for 1,3-butadiene catalytic hydrogenation over the biosynthesized Pd/γ-Al_2O_3 catalysts at low temperature, and the coexistence of small amount of oxidation state PdO/Pd^{2+} was beneficial for the butene selectivity.

Acknowledgements

This work was supported by the National Natural Science Foundation of China (21536010), and the Natural Science Foundation of Fujian Province (2017J01025).

Notes and references

1 R. Hou, M. D. Porosoff, J. G. Chen and T. Wang, *Appl. Catal. A-Gen.*, 2015, **490**, 17-23.
2 C. Deraedt, G. Melaet, W. T. Ralston, R. Ye and G. A. Somorjai, *Nano Lett*, 2017, **17**, 1853-1862.
3 A. Hugon, L. Delannoy, J.-M. Krafft and C. Louis, *J. Phys. Chem. C*, 2010, **114**, 10823-10835.
4 S. Chen, L. Meng, B. Chen, W. Chen, X. Duan, X. Huang, B. Zhang, H. Fu and Y. Wan, *ACS Catal.*, 2017, **7**, 2074-2087.
5 G. X. Pei, X. Y. Liu, A. Wang, L. Li, Y. Huang, T. Zhang, J. W. Lee, B. W. L. Jang and C. Y. Mou, *New J. Chem.,* 2014, **38**, 2043-2051.
6 B. Bachiller-Baeza, J. Peña-Bahamonde, E. Castillejos-López, A. Guerrero-Ruiz and I. Rodríguez-Ramos, *Catal. Today*, 2015, **249**, 63-71.
7 J. Liu, H. Wang, Y. Chen, M. Yang and Y. Wu, *Catal. Commun.*, 2014, **46**, 11-16.
8 A. Abd El-Moemen, A. M. Abdel-Mageed, J. Bansmann, M. Parlinska-Wojtan, R. J. Behm and G. Kučerová, *J. Catal.*, 2016, **341**, 160-179.
9 G. S. Wang, J. W. Lee and C. K. Sang, *Appl. Catal. B Environ.*, 2008, **84**, 133–141.
10 P. Dégé, L. Pinard, P. Magnoux and M. Guisnet, *Appl. Catal. B Environ.*, 2000, **27**, 17-26.
11 S. Huang, C. Zhang and H. He, *Catal. Today*, 2008, 139, 15-23.
12 X. Zhang, Z. Qu, F. Yu, Y. Wang and X. Zhang, *J. Mol. Catal. A-Chem.*, 2013, **370**, 160-166.
13 L. C. Wang, L. He, Y. M. Liu, Y. Cao, H. Y. He, K. N. Fan and J. H. Zhuang, *J. Catal.*, 2009, **264**, 145-153.
14 G. Suresh, J. Radnik, V. N. Kalevaru, M. M. Pohl, M. Schneider, B. Lücke, A. Martin, N. Madaan and A. Brückner, *Phy. Chem. Chem. Phy.*, 2010, **12**, 4833.
15 Q. Zhang, L. Ma, C. Lu, X. Xu, J. Lyu and X. Li, *React. Kinet. Mech. Catal.*, 2015, **114**, 629-638.
16 F. Skoda, M. P. Astier, G. M. Pajonk and M. Primet, *React. Kinet. Mech. Catal.*, 1995, **55**, 101-110.
17 E. Sasmaz, C. Wang, M. J. Lance and J. Lauterbach, *J. Mater. Chem. A*, 2017. **5**, 12998-13008.
18 H. Zhu, Z. Qin, W. Shan, W. Shen and J. Wang, *J. Catal.*, 2005, **233**, 41-50.
19 S. Huang, C. Zhang and H. He, *J. Environ. Sci.*, 2013, **25**, 1206-1212.
20 V. V. Chesnokov, I. P. Prosvirin, V. I. Zaikovskii and N. A. Zaitseva, *Eurasian Chem. Technol. J.*, 2016, **5**, 127.
21 I. Saldan, Y. Semenyuk, I. Marchuk and O. Reshetnyak, *J. Mater. Sci.*, 2015, **50**, 2337-2354.
22 M. Du, D. Sun, H. Yang, J. Huang, X. Jing, T. Odoom-Wubah, H. Wang, L. Jia and Q. Li, *J. Phy. Chem. C*, 2014, **118**, 19150-19157.
23 F. Yang, X. L. Jing, J. L. Huang, D. H. Sun and Q. B. Li, *Ind. Eng. Chem. Res.*, 2015, **54**, 5373-5380.
24 G. Zhan, M. Du, J. Huang and Q. Li, *Catal. Commun.*, 2011, **12**, 830-833.
25 J. L. Huang, L. Q. Lin, Q. B. Li, D. H. Sun, Y. P. Wang, Y. H. Lu, N. He, K. Yang, X. Yang, H. X. Wang, W. T. Wang and W. S. Lin, *Ind. Eng. Chem. Res.*, 2008, **47**, 6081-6090.
26 M. Du, G. Zhan, X. Yang, H. Wang, W. Lin, Y. Zhou, J. Zhu, L. Lin, J. Huang, D. Sun, L. Jia and Q. Li, *J. Catal.*, 2011, **283**, 192-201.
27 N. S. Babu, N. Lingaiah and R. Gopinath, *J. Phys. Chem. C*, 2007, **111**, 6447-6453.
28 K. Shanthi, B. Viswanathan, P. Selvam, P. Sangeetha and K. S. R. Rao, *Appl. Catal. A-Gen.*, 2009, **353**, 160-165.
29 P. K. Rao, K. S. R. Rao and A. H. Padmasri, *Cattech.*, 2003, **7**, 218-225.
30 R. Gholami and K. J. Smith, *Appl. Catal. B-Environ.*, 2015, **168–169**, 156-163.
31 L. Ouyang, P. F. Tian, G. J. Da, X. C. Xu, C. Ao, T. Y. Chen, R. Si, J. Xu and Y. F. Han, *J. Catal.*, 2015, **321**, 70-80.
32 F. Wang, K. Zhao, H. Zhang, Y. Dong, T. Wang and D. He, *Chem. Eng. J.*, 2014, **242**, 10-18.
33 Y. Cao, R. Ran, X. Wu, B. Zhao, J. Wan, D. Weng, Y. Cao, B. Zhao, J. Wan and D. Weng, *Appl. Catal. A-Gen.*, 2013, **457**, 52-61.
34 A. Borodziński and G. C. Bond, *Catal. Rev.*, 2006, **48**, 91-144.
35 G. Zhang, M. Du, Q. Li, X. Li, J. Huang, X. Jiang and D. Sun, *RSC Adv.*, 2013, **3**, 1878.
36 N. E. Kolli, L. Delannoy and C. Louis, *J. Catal.*, 2013, **297**, 79-92.

View Article Online
DOI: 10.1039/C7NJ02557B

37 K. Pattamakomsan, E. Ehret, F. Morfin, P. Gélin, Y. Jugnet, S. Prakash, J. C. Bertolini, J. Panpranot and F. J. C. S. Aires, *Catal. Today*, 2011, **164**, 28-33.
38 D. Tessier, A. Rakai and F. o. Bozon-Verduraz, *J. Chem. Soc. Faraday Trans.*, 1992, **88**, 741-749.
39 G. D. Gatta, B. Fubini, G. Ghiotti and C. Morterra, *J. Catal.*, 1976, **43**, 90-98.
40 K. Pattamakomsan, F. J. C. S. Aires, K. Suriye and J. Panpranot, *React. Kinet. Mech. Catal.*, 2011, **103**, 405-417.
41 C. Liu, K. Yang, J. Zhao, Y. Pan and D. Liu, *Catal. Commun.*, 2015, **67**, 72-77.

View Article Online
DOI: 10.1039/C7NJ02557B

Graphic abstract:

Effect of pretreatment atmosphere on 1,3-butadiene hydrogenation over biosynthesized Pd/γ-Al_2O_3 catalysts was reported.